

# Microstructure, ferromagnetism, and magnetic transport of $\text{Ti}_{1-x}\text{Co}_x\text{O}_2$ amorphous magnetic semiconductor

Hong-Qiang Song,<sup>a)</sup> Liang-Mo Mei, and Shi-Shen Yan

*School of Physics and Microelectronics, Shandong University, Jinan, Shandong 250100, People's Republic of China and National Key Laboratory of Crystal Materials, Shandong University, Jinan, Shandong 250100, People's Republic of China*

Xiu-Liang Ma

*Shenyang National Laboratory for Materials Science, Institute of Metal Research, Chinese Academy of Sciences, Shenyang, Liaoning 110016, People's Republic of China*

Jia-Ping Liu

*Department of Physics, The University of Texas at Arlington, Box 19059, Arlington, Texas 76019*

Yong Wang and Ze Zhang

*Beijing National Laboratory for Condensed Matter Physics, Institute of Physics, Chinese Academy of Sciences, Beijing 100080, People's Republic of China*

(Received 26 November 2005; accepted 11 April 2006; published online 22 June 2006)

$\text{TiO}_2$ -based magnetic semiconductors with high Co doping concentrations ( $\text{Ti}_{1-x}\text{Co}_x\text{O}_2$ ) were synthesized under thermal nonequilibrium condition by sputtering machine. Microstructure and composition analysis by transmission electron microscopy, x-ray photoelectron spectroscopy, and electron energy-loss spectroscopy indicated that Co element was incorporated into  $\text{TiO}_2$  to form  $\text{Ti}_{1-x}\text{Co}_x\text{O}_2$  compound. The direct evidence for the compositional inhomogeneity of the  $\text{Ti}_{1-x}\text{Co}_x\text{O}_2$  compound was given. Room temperature ferromagnetism with high magnetization was obtained, which could be attributed to the intrinsic properties of the amorphous magnetic semiconductor. The electrical transport in a low temperature range was explained by spin-dependent Efros's variable range hopping, and correspondingly an exponential function of the magnetoresistance versus  $T^{-1/2}$  was found. © 2006 American Institute of Physics. [DOI: 10.1063/1.2204758]

## I. INTRODUCTION

Since the room temperature ferromagnetism was found in Co-doped  $\text{TiO}_2$  (Ref. 1) magnetic semiconductor, magnetic semiconductors have been extensively studied<sup>2-12</sup> for their great importance in spintronics devices. For the  $\text{TiO}_2$ -based room temperature magnetic semiconductors, some researchers believed that the ferromagnetism originates from the Co metal clusters<sup>3,5,6,11</sup> embedded in  $\text{TiO}_2$ , but now most researchers tend to believe that the ferromagnetism is the intrinsic property of  $\text{Ti}_{1-x}\text{Co}_x\text{O}_2$  magnetic semiconductors.<sup>1,2,4,7,12</sup> However, the origin of the weak ferromagnetism at room temperature is still an open question. Moreover, in these investigations, the Co doping concentrations in  $\text{TiO}_2$  were usually limited to a few percents,<sup>1-8</sup> and the observed saturation magnetization was very small.

The magnetoresistance of magnetic semiconductors was also of great importance for spintronics devices. Recently, a large magnetoresistance was found in the inhomogeneous  $\text{Zn}_{1-x}\text{Co}_x\text{O}_{1-v}$  magnetic semiconductor at room temperature<sup>10</sup> although the magnetoresistance usually appears at very low temperature<sup>1,4,8</sup> for low doping concentration in magnetic semiconductors. In the system with strong chemical inhomogeneity on the subnanometer scale, such as  $\text{Zn}_{1-x}\text{Co}_x\text{O}_{1-v}$  ( $v$ =vacancy) inhomogeneous compound mag-

netic semiconductor<sup>10</sup> of high Co concentration, there are many defects such as the doped Co atoms, O vacancies, and Zn interstitials if the ZnO was regarded as a host material. This compositional inhomogeneity will produce strong local potential and lead to Anderson localization of the carriers near the Fermi level, which will significantly influence the electrical transport and magnetoresistance. However, the electrical transport and the magnetoresistance in the inhomogeneous magnetic semiconductors are still less known.

The intrinsic chemical inhomogeneity in the form of "clustered states"<sup>13-15</sup> has been regarded as a common feature of magnetic semiconductors, colossal magnetoresistance manganites,<sup>16</sup> and high temperature superconducting cuprates. The special chemical inhomogeneity has been found in Mn-doped Ge ferromagnetic semiconductors,<sup>17</sup> which show Mn-rich and Mn-depleted phases, rather than in metallic Mn clusters. On the other hand, using the first-principles density-functional approaches, impurity distributions and magnetic properties of Co-doped anatase  $\text{TiO}_2$  were investigated.<sup>18</sup> From the total energies calculated for various possible configurations, Co atoms were found to prefer the nonuniform doping mode with short Co-Co distances. This nonuniform distribution furthermore is crucial for the ferromagnetic ordering observed in  $\text{Ti}_{1-x}\text{Co}_x\text{O}_2$ , whereas the antiferromagnetic state prevails in uniformly doped cases in-

<sup>a)</sup>Electronic mail: tianqin@mail.sdu.edu.cn

vestigated ( $x=0.0625$ ). But to date no direct experimental evidence on the compositional inhomogeneity of the oxide-based semiconductors has been given.

Comparing various experimental results from different research groups, it is easy to find that the magnetic and electric transport properties of magnetic semiconductors doped with transitional metal elements are very sensitive to the concentration, distribution, and valence of the transitional metal elements, which were associated with the synthesis methods and postprocesses.<sup>2</sup> We believe that different synthesis methods and postprocesses will result in different compositions and microstructures, which finally determine the electronic and magnetic properties. Therefore, various magnetic properties observed by different groups may have different origins. This means that both intrinsic and extrinsic origins are possible even for the same material system, depending on the composition and microstructure. Therefore, a systematic study on the synthesis, microstructure, magnetism, and magnetic transport is necessary for the magnetic semiconductors.

In this paper, we reported  $\text{Ti}_{1-x}\text{Co}_x\text{O}_2$  magnetic semiconductor of high Co doping concentration. This material is in an amorphous state in contrast with the common single crystal or polycrystal. Direct evidence on the compositional inhomogeneity was given. More interestingly, this material shows a high magnetization, spin-dependent Efros's variable range hopping, and large magnetoresistance.

## II. EXPERIMENTS

$\text{Ti}_{1-x}\text{Co}_x\text{O}_2$  amorphous magnetic semiconductor films were prepared on glass substrates by alternately sputtering very thin Co and  $\text{TiO}_2$  layers for 60 periods at room temperature, i.e., the nominal structure is  $(\text{Co } 0.6 \text{ nm}/\text{TiO}_2 \text{ } 0.5\text{--}2 \text{ nm}) \times 60$ , which forms  $\text{Ti}_{1-x}\text{Co}_x\text{O}_2$  in the Ar and background  $\text{O}_2$  gas due to atomic interdiffusion. Finally 2 nm  $\text{TiO}_2$  was deposited as protective layer.

The microstructures of  $\text{Ti}_{1-x}\text{Co}_x\text{O}_2$  films were observed in cross-section view by transmission electron microscopy (TEM) equipped with energy dispersive x-ray spectroscopy (EDS). The magnetic properties were measured by a superconducting quantum interference device (SQUID) system from 5 K to room temperature. The electrical transport and the magnetoresistance were measured in Van der Pauw configuration by a physical property measurement system (PPMS). For both magnetism and magnetoresistance measurements, the magnetic field is applied in the film plane. Although the samples with various  $\text{Ti}_{1-x}\text{Co}_x\text{O}_2$  compositions were prepared, here we mainly reported the experimental results of  $\text{Ti}_{0.24}\text{Co}_{0.76}\text{O}_2$  sample due to the similarity in physical properties for these samples.

## III. EXPERIMENTAL RESULTS AND DISCUSSION

Figure 1(a) is a low magnification TEM micrograph of the as-deposited film in cross-section view. The weak and uniform contrast indicates that the composition of the sample is nearly uniform on a large scale. The quantitative analysis of EDS shows about 24 at. % Ti and 76 at. % Co within the film. The high-resolution TEM image [Fig. 1(b)] also shows a weak and uniform contrast without well defined grain

boundaries and clear crystalline. It is clear that the  $\text{Ti}_{0.24}\text{Co}_{0.76}\text{O}_2$  film is in an amorphous state. The inset in Fig. 1(a) is the corresponding electron diffraction pattern, which exhibits a diffuse ring, indicating an amorphous structure.

Figure 1(c) is the corresponding elemental mapping image of Co taken in the same place of Fig. 1(b). In order to show the compositional inhomogeneity, the mapping image of Co was obtained by choosing a proper contrast so that the bright points or very small areas in the image only show the Co-rich areas. It can be clearly seen that the distribution of Co atoms is inhomogeneous on the subnanometer scale. However, there is no any pure Co metal cluster within the whole films. By contrast, after the films were annealed at 300 °C, many Co crystalline particles were formed and could be seen clearly (not shown).

In order to further check if there exist pure Co clusters in the as-deposited samples, x-ray photoelectron spectroscopy (XPS) experiments were carried out in a vacuum chamber. The samples were loaded into a MICROLAB MK II x-ray photoelectron spectroscopy system. A Mg  $K\alpha$  line at 1253.6 eV was used with the x-ray source run at 14.5 kV. An energy analyzer was operated at a constant pass energy of 50 eV, which resulted in an energy resolution of about 0.6 eV. Since XPS is mainly sensitive to the sample surface, the sample was etched by  $\text{Ar}^+$  in the vacuum chamber of XPS for several times to get the XPS signals from different deepness of the sample. We got the same XPS results at different deepnesses of the sample. Figure 1(d) shows the XPS of the Co element in  $\text{Ti}_{0.24}\text{Co}_{0.76}\text{O}_2$  film. In Fig. 1(d), the energy difference between Co  $2p_{3/2}$  and Co  $2p_{1/2}$  is 15.35 eV, which excludes the possibility of the formation of Co metal clusters because the energy difference for Co metal clusters is 15.05 eV (Ref. 19) (we obtained 15.00 eV for the Co film). However, since the energy resolution of the XPS is not high enough for the present experiments, it is hard to make more detailed analysis.

The chemical states of Co element were further explored by electron energy-loss spectroscopy (EELS) on FEI's transmission electron microscopy Tecnai F30. Figures 1(e) and 1(f) show  $L_3$  and  $L_2$  edges in an EEL spectrum of the sample, which were recorded in image mode. The white line ratio (the intensity ratio of  $L_3/L_2$ ) was used to qualitatively measure the chemical states of transition metal atoms. The white line ratio varies from 3.6 to 3.7 for different detecting regions, which corresponds to the compositional inhomogeneity in the sample. It was reported that the white line ratios for Co element in  $\text{Co}_{52}\text{Al}_{20}\text{O}_{28}$  and  $\text{Co}_{36}\text{Al}_{22}\text{O}_{42}$  oxides are 3.6 and 3.7, respectively.<sup>20</sup> This means that the chemical valence of Co element in the  $\text{Ti}_{0.24}\text{Co}_{0.76}\text{O}_2$  film is close to those observed in the  $\text{Co}_{52}\text{Al}_{20}\text{O}_{28}$  and  $\text{Co}_{36}\text{Al}_{22}\text{O}_{42}$  oxides. By contrast, for pure Co thin films prepared by vacuum deposition, the white line ratio is only 3.3.<sup>20</sup> Therefore, the present  $\text{Ti}_{0.24}\text{Co}_{0.76}\text{O}_2$  sample should be regarded as an inhomogeneous compound, excluding the existence of the pure Co clusters.

Figure 2(a) shows hysteresis loops measured at 5 and 290 K, respectively, and the inset shows the details of the  $M$ - $H$  loop measured in the low field region at 290 K. The ferromagnetism is clearly shown by the coercivity, rema-

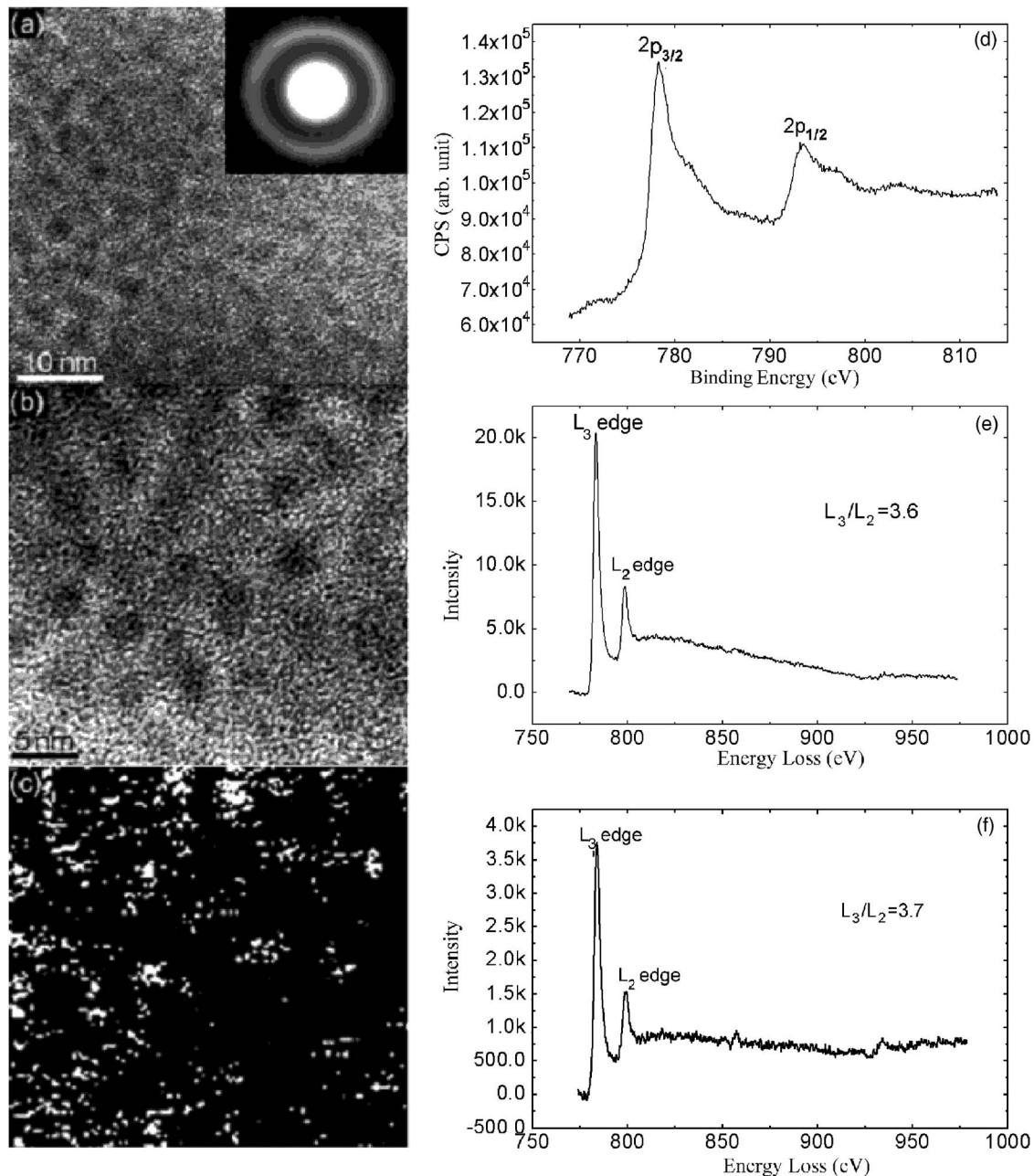


FIG. 1. (a) A low magnification micrograph of the as-deposited sample and the corresponding electron diffraction pattern in the inset. (b) The HRTEM image and (c) the corresponding elemental mapping of Co. (d) XPS of Co  $2p_{3/2}$  and Co  $2p_{1/2}$  peaks. [(e) and (f)] EELS of  $\text{Ti}_{0.24}\text{Co}_{0.76}\text{O}_2$  films.

nence, and low saturation field. Figure 2(b) shows the temperature dependence of the net saturation magnetization of the sample, the substrate signals, and the total signals measured in  $3 \times 10^4$  Oe magnetic field. In Fig. 2(b), the net saturation magnetization of the sample reduces very slowly with increasing temperature from 5 to 290 K, indicating that the Curie temperature is above 290 K. The magnetization of  $\text{Ti}_{0.24}\text{Co}_{0.76}\text{O}_2$  is  $524 \text{ emu/cm}^3$  ( $1.29 \mu_B/\text{Co}$ ) at 5 K and  $503 \text{ emu/cm}^3$  ( $1.24 \mu_B/\text{Co}$ ) at 290 K.

As for the origin of the ferromagnetism, it can be explained as intrinsic ferromagnetism. In the amorphous  $\text{Ti}_{0.24}\text{Co}_{0.76}\text{O}_2$  magnetic semiconductor with chemical composition inhomogeneity, there are many defects such as the doped Co atoms, O vacancies, and Ti interstitials as compared with the crystalline  $\text{TiO}_2$  host material. The defect lev-

els can supply  $s$ ,  $p$  carrier electrons and lead to the spin-spin exchange interaction between the  $s$ ,  $p$  carrier electrons and localized  $d$  electrons of Co. There also exist direct  $d-d$  exchanges interaction between the neighbor Co atoms due to the high Co concentration. Therefore, in this system, local Co atoms may establish local ferromagnetic structure and even long ranged ferromagnetic structure through  $sp-d$  interaction and direct  $d-d$  exchange interaction between the neighbor Co atoms.

Figures 3(a) and 3(b) show the dependence of the sheet resistance  $R$  and the magnetoresistance (MR) ratio on the magnetic field, measured at 5 and 290 K, respectively. The MR ratio is defined as  $\text{MR}(H, T) = \{ [R(H_s, T) - R(H, T)] / R(H_s, T) \} \times 100\%$  where  $R(H, T)$  is the resistance at field  $H$  and temperature  $T$  and  $R(H_s, T)$  is the resistance

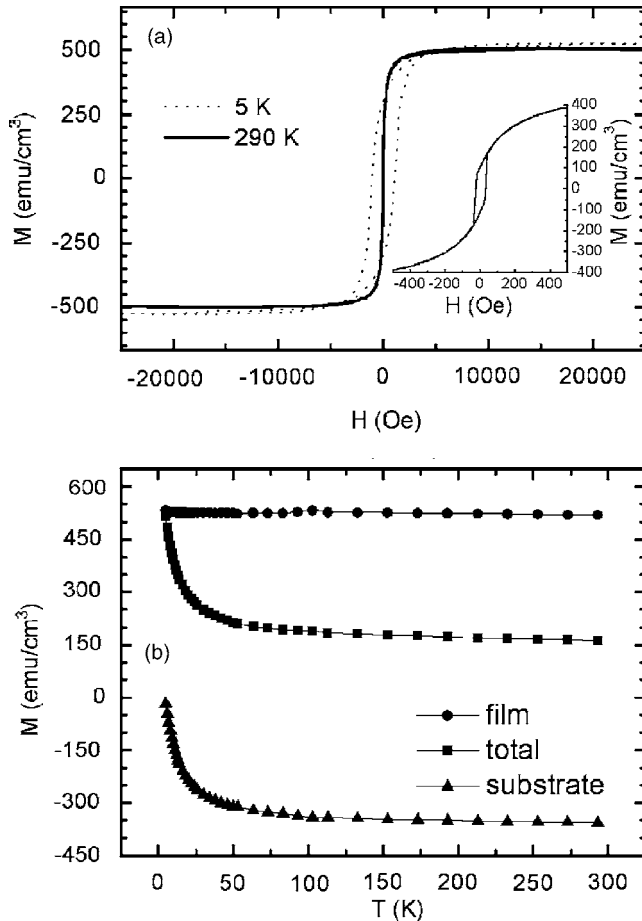


FIG. 2. (a) Hysteresis loops measured at 5 and 290 K, respectively. The inset is the low field hysteresis loop measured at 290 K. (b) The temperature dependence of the net saturation magnetization of the sample, the substrate signals, and the total signals measured in  $3 \times 10^4$  Oe field.

the maximum field  $H_s$  ( $H_s = 5 \times 10^4$  Oe in our experiments). The  $\text{Ti}_{0.24}\text{Co}_{0.76}\text{O}_2$  samples show a large negative magnetoresistance at a relatively small field in the temperature range from 5 to 290 K, such as 12.5% at 5 K for the MR peak and 4.6% at 290 K. Similar negative magnetoresistance was also observed when the applied field is perpendicular to the film plane, such as 12.0% at 5 K and 4.5% at 290 K. The  $R$ - $H$  curves in Fig. 3(a) show an obvious magnetic hysteresis behavior, which corresponds to the magnetic hysteresis of the  $M$ - $H$  loop in Fig. 2(a). This implies that the negative magnetoresistance observed in Fig. 3 is related to spin-dependent effects of ferromagnetic materials.

Figure 4(a) shows the  $R$ - $T$  curves (sheet resistance  $R$  and temperature  $T$ ) at  $H_s = 5 \times 10^4$  Oe field and without field (the initial demagnetized state), and Fig. 4(b) shows the corresponding  $\ln R$ - $T^{-1/2}$  relation. It is clear that the sheet resistance monotonously increases with decreasing temperature. This is a typical feature of the electrical transport of semi-conducting materials. More interestingly, the linear relationship between  $\ln R$  and  $T^{-1/2}$  was found in a low temperature range below 80 K for the two curves, i.e.,

$$\ln R(H, T) = A(H) + B(H)/T^{1/2} \quad (1)$$

or

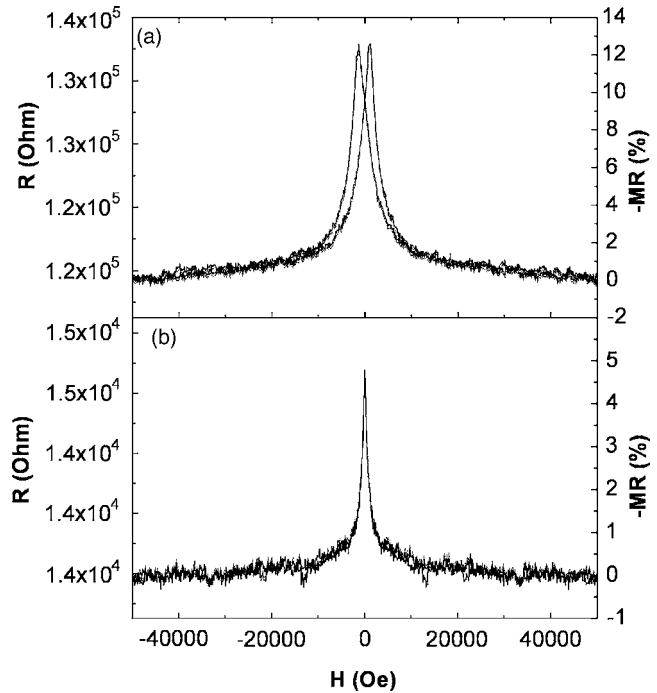


FIG. 3. Dependence of the sheet resistance  $R$  and the MR ratio on the magnetic field measured at 5 K (a) and 290 K (b), respectively.

$$R(H, T) = R_0(H) \exp\{[T_0(H)/T]^{1/2}\}, \quad (2)$$

where  $A(H)$  and  $B(H)$  are two coefficients which correspond to the intersection and slope of the extrapolated lines, respectively. In Eq. (2),  $R_0(H) = \exp[A(H)]$  and  $T_0(H) = [B(H)]^2$ . From the linear fitting, we get  $A(0) = 9.52708[\ln(\text{ohm})]$  and  $B(0) = 5.00334(\text{K}^{1/2})$  for the  $R$ - $T$  curve without field, and  $A(H_s) = 9.48011[\ln(\text{ohm})]$  and  $B(H_s) = 4.88027(\text{K}^{1/2})$  for  $R$ - $T$  curve at  $H_s = 5 \times 10^4$  Oe.

According to the definition of MR and Eq. (2), we can obtain the expression of MR when the field is swept from the initial demagnetized state to  $H_s = 5 \times 10^4$  Oe,

$$\text{MR} = 1 - C_0 \exp(D_0/T^{1/2}), \quad (3)$$

where  $C_0 = \exp[A(0) - A(H_s)] = \exp(0.04697) = 1.0481$  and  $D_0 = B(0) - B(H_s) = 0.12307 \text{ K}^{1/2}$ . Figure 4(c) shows the temperature dependence of the experimental MR ratio and the theoretical results of Eq. (3). The negative MR decreases very quickly with increasing temperature in a low temperature range, and the experimental results and theoretical fitting are in very good agreement. In high temperature range above 80 K, the MR decreases very slowly with increasing temperature, but Eqs. (2) and (3) do not work in this temperature range.

It is well known that in the disordered, inhomogeneous, or amorphous systems,  $R \propto \exp[(T_0/T)^{1/2}]$  relation is called Efros's variable range hopping.<sup>21</sup> However, the mechanism of the large negative magnetoresistance in the variable range hopping region is still less known. We believe that it can be explained as the spin-dependent variable range hopping.<sup>22,23</sup> In the  $\text{Ti}_{0.24}\text{Co}_{0.76}\text{O}_2$  magnetic semiconductor system, there are strong spin-spin exchange interactions among the carrier spins and the local spins in addition to electron-electron Coulomb interaction. In the magnetic field,

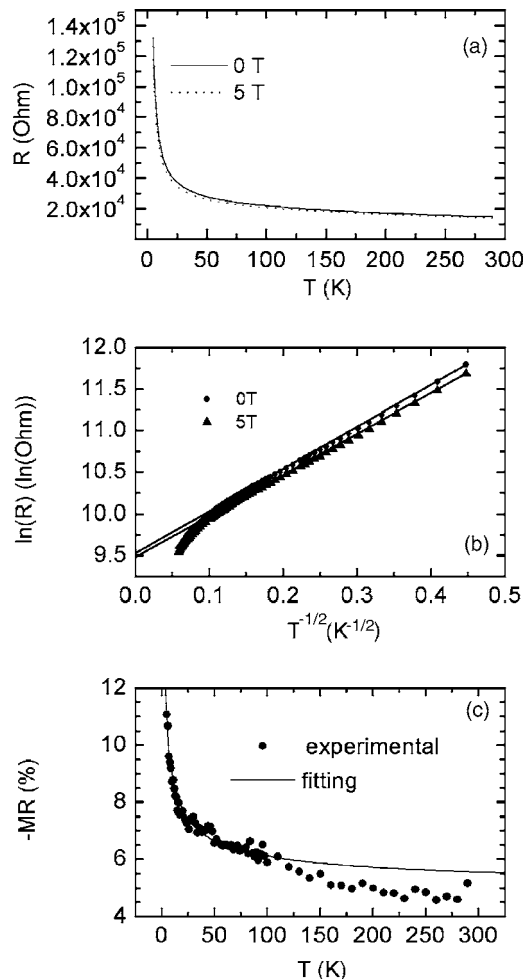


FIG. 4. (a) Temperature dependence of the sheet resistance  $R$ . (b) The  $\ln R-T^{-1/2}$  relation. (c) Temperature dependence of the MR ratio and the theoretical calculation according to Eq. (3).

the spins tend to align parallel, and the spin-spin exchange energy becomes small. As a result, the variable range hopping electrons have a less resistance, showing spin-dependent variable range hopping and large negative magnetoresistance.

#### IV. CONCLUSIONS

In summary,  $\text{Ti}_{0.24}\text{Co}_{0.76}\text{O}_2$  inhomogeneous amorphous magnetic semiconductors were synthesized. Microstructure and composition analysis indicated that Co element was in-

corporated into  $\text{TiO}_2$  to form  $\text{Ti}_{1-x}\text{Co}_x\text{O}_2$  compound. The direct evidence for the compositional inhomogeneity of the  $\text{Ti}_{1-x}\text{Co}_x\text{O}_2$  compound was given. The room temperature ferromagnetism with high magnetization was obtained. The magnetic transport shows the spin-dependent Efros's variable range hopping behavior in the low temperature range below 80 K. Correspondingly, the exponential function of the magnetoresistance versus  $T^{-1/2}$  was deduced.

#### ACKNOWLEDGMENTS

The authors are grateful to Qi-Kun Xue and Kan Xie for XPS measurements at Institute of Physics, CAS. This work was supported by the State Key Project of Fundamental Research (Grant No. 2001CB610603), the National Natural Science Foundation of China (Grant Nos. 10234010, 50102019, and 50572053), and New Century Fund for Outstanding Scholars (Grant No. 040634).

- <sup>1</sup>Y. Matsumoto *et al.*, *Science* **291**, 854 (2001).
- <sup>2</sup>S. A. Chambers *et al.*, *Appl. Phys. Lett.* **79**, 3467 (2001).
- <sup>3</sup>D. H. Kim *et al.*, *Appl. Phys. Lett.* **81**, 2421 (2002).
- <sup>4</sup>S. R. Shinde *et al.*, *Phys. Rev. B* **67**, 115211 (2003).
- <sup>5</sup>S. A. Chambers, T. Droubay, C. M. Wang, A. S. Lea, R. F. C. Farrow, L. Folks, V. Deline, and S. Anders, *Appl. Phys. Lett.* **82**, 1257 (2003).
- <sup>6</sup>J.-Y. Kim *et al.*, *Phys. Rev. Lett.* **90**, 017401 (2003).
- <sup>7</sup>A. Manivannan, G. Glaspell, and M. S. Seehra, *J. Appl. Phys.* **94**, 6994 (2003).
- <sup>8</sup>Z. J. Wang, J. K. Tang, L. D. Tung, W. L. Zhou, and L. Spinu, *J. Appl. Phys.* **93**, 7870 (2003).
- <sup>9</sup>J. H. Kim, H. Kim, D. Kim, Y. E. Ihm, and W. K. Choo, *J. Appl. Phys.* **92**, 6066 (2002).
- <sup>10</sup>S. S. Yan *et al.*, *Appl. Phys. Lett.* **84**, 2376 (2004).
- <sup>11</sup>P. A. Stampe, R. J. Kennedy, Y. Xin, and J. S. Parker, *J. Appl. Phys.* **93**, 7864 (2003).
- <sup>12</sup>Z. Wang, J. Tang, Y. Chen, L. Spinu, W. Zhou, and L. D. Tung, *J. Appl. Phys.* **95**, 7384 (2004).
- <sup>13</sup>G. Alvarez and E. Dagotto, *J. Magn. Magn. Mater.* **15**, 272 (2004).
- <sup>14</sup>C. Timm, F. Schäfer, and F. von Oppen, *Phys. Rev. Lett.* **89**, 137201 (2002).
- <sup>15</sup>G. Alvarez, M. Mayr, and E. Dagotto, *Phys. Rev. Lett.* **89**, 277202 (2002).
- <sup>16</sup>T. Becker, C. Streng, Y. Luo, V. Moshnyaga, B. Damaschke, N. Shannon, and K. Samwer, *Phys. Rev. Lett.* **89**, 237203 (2002).
- <sup>17</sup>J.-S. Kang *et al.*, *Phys. Rev. Lett.* **94**, 147202 (2005).
- <sup>18</sup>Z. Yang, G. Liu, and R. Wu, *Phys. Rev. B* **67**, 060402R (2003).
- <sup>19</sup>H.-Jun Lee, S.-Y. Jeong, C.R. Cho, and C. H. Park, *Appl. Phys. Lett.* **81**, 4020 (2002).
- <sup>20</sup>N. Tanaka, J. Yamasaki, S. Mitani, and K. Takanashi, *Scr. Mater.* **48**, 909 (2003).
- <sup>21</sup>A. L. Efros and B. I. Shklovskii, *J. Phys. C* **8**, L49 (1975).
- <sup>22</sup>M. Viret, L. Ranno, and J. M. D. Coey, *Phys. Rev. B* **55**, 8067 (1997).
- <sup>23</sup>P. Wagner, I. Gordon, L. Trappeniers, J. Vanacken, F. Herlach, V. V. Moshchalkov, and Y. Bruynseraede, *Phys. Rev. Lett.* **81**, 3980 (1998).